RSC Advances

ROYAL SOCIETY OF CHEMISTRY

www.rsc.org/advances

Journal Name

ARTICLE

Slow magnetic relaxation of a three-dimensional metal-organic framework featuring a unique dysprosium(III) oxalate layer

Received 00th January 20xx,
Accepted 00th January 20xx

DOI: 10.1039/x0xx00000x

www.rsc.org/

Cai-Ming Liu,[a,*] De-Qing Zhang,[a] and Dao-Ben Zhu[a]

A novel lanthanide metal-organic framework was yielded by hydrothermal reaction of 5-chloro-6-hydroxypyridine-3-carboxylic acid (5-Cl-6-HOPy-3-CO_2H) and Dy_2O_3 in the presence of oxalic acid [$H_2(OX)$], namely, [Dy_2(1H-5-Cl-6-Opy-3-CO_2)$_2$(OX)$_2$(H_2O)$_3$]·2.5 H_2O (**1**, 1H-5-Cl-6-Opy-3-CO_2^- = 1-hydro-5-chloro-6-oxopyridine-3-carboxylate, which was formed in the autoisomerization of single deprotonated 1H-5-Cl-6-HOpy-3-CO_2^- anion). The dysprosium(III) ions are bridged by oxalate anions to construct an interesting 4-connected layer network with a Schälfli topology symbol of ($3^2.5^2$)(3.5^3), such layers are connected with each other by the 1H-5-Cl-6-HOpy-3-CO_2^- anions to form a three-dimensional framework. Magnetic investigations indicated that **1** is a field-induced single-molecule magnet, displaying two-step thermal magnetic relaxation, with an effective thermal barrier of 37.6 K. Surprisingly, a zigzag chain-like gadolinium(III) complex, [Gd(1H-5-Cl-6-Opy-3-CO_2)$_2$(OX)(H_2O)$_3$]·2.5 H_2O (**2**), was isolated using Gd_2O_3 instead of Dy_2O_3 owing to the lanthanide contraction effect. Notebaly, a unique F-shaped $(H_2O)_6$ supramolecular aggregate exists in the crystal structure of **2**.

Introduction

Lanthanide metal–organic frameworks (LnMOFs), a special class of molecular materials known as metal–organic frameworks constructed from trivalent lanthanides, have attracted increasing interest in numerous research fields such as lighting, optical communications, photonics, biomedical devices, catalysis, adsorption, magnetic materials, separation sensors and luminescent sensors.[1] They can even serve as multifunctional materials combining light emission with other properties such as microporosity, magnetism, chirality, molecule and ion sensing, and catalysis.[2] One feasible strategy for assembly of LnMOFs is to utilize carboxylic acids as organic linkers due to not only their rich binding modes but also the lanthanide ions' high affinity for the carboxylate oxygen atoms. Remarkably, oxalic acid was often combined with the carboxylic acids to construct novel LnMOFs.[3]

On the other hand, the discovery of Mn_{12} single-molecule magnet(SMM) in 1993 is a milestone in the field of molecular magnets.[4] The SMMs show magnetic bistability below the blocking temperature(T_B), which can be potentially used in high-technique fields such as high-density information storage, quantum computer and spintronics.[5] Generally, the nature of the SMM behaviours requires a molecule to possess not only a large spin ground state (*S*) but also a negative uniaxial magnetic anisotropy (*D*). The lanthanide ions such as the Dy^{3+} ion, which have large magnetic moments and remarkable magnetic anisotropy, thus become excellent components of the SMMs. Although most of lanthanide-based SMMs(LnSMMs) are cluster complexes and single-ion compounds, recent researches indicated that the SMM behaviours also exist in some high-dimensional molecular systems,[6] because the magnetic exchange interaction among the lanthanide ions mediated by the organic linkers is too weak to be considered. However, in contrast to abundant luminescent LnMOFs, the LnMOF-SMMs are still at an early stage of development.

Our recent interest is also directed toward the architecture of new LnMOFs[7] and new LnSMMs.[6i,6j,8] Recently, we used 6-hydroxypyridine-3-carboxylic acid (6-HOPy-3-CO_2H) as the main organic linker to construct several LnMOFs (Ln = Nd^{3+}, Sm^{3+}, Eu^{3+} and Gd^{3+}) under hydrothermal conditions, which show attractive topologies and optical and/or magnetic properties.[7a,7b] However, the attempt to assembly the corresponding DyMOFs was failed. We thus chose its derivative 5-chloro-6-hydroxypyridine-3-carboxylic acid (5-Cl-6-HOPy-3-CO_2H) as the main ligand and the oxalate as the co-ligand to prepare the DyMOFs. Herein we describe a novel 3D DyMOF with an interesting dysprosium(III) oxalate layer, [Dy_2(1H-5-Cl-6-Opy-3-CO_2)$_2$(OX)$_2$(H_2O)$_3$]·2.5 H_2O (**1**, 1H-5-Cl-6-Opy-3-CO_2^- = 1-hydro-5-chloro-6-oxopyridine-3-carboxylate), which displays field-induced two-step thermal magnetic relaxation. Comparably, the corresponding gadolinium(III) complex, [Gd(1H-5-Cl-6-Opy-3-CO_2)$_2$(OX)(H_2O)$_3$]·2.5H_2O (**2**), is a one-dimensional (1D) zigzag chain-like compound. Notably, the new ligand, 1H-5-Cl-6-Opy-3-CO_2^- anion, was generated by an autoisomerization from the enol form into the ketone form.

[a] Beijing National Laboratory for Molecular Sciences, Center for Molecular Science, Key Laboratory of Organic Solids, Institute of Chemistry, Chinese Academy of Sciences, Beijing 100190, P. R. China; E-mail: cmliu@iccas.ac.cn

Electronic Supplementary Information (ESI) available: X-ray crystallographic data for complexes **1** and **2** in CIF format, CCDC 1406623-1406624. Additional magnetic characterization (Figures S1–S7 and Tables S1 and S2). See DOI: 10.1039/x0xx00000x

of the single deprotonated 5-Cl-6-HOPy-3-CO_2^- anion (Scheme 1).

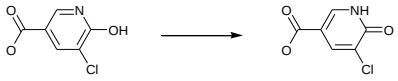

Scheme 1. Autoisomerization of the single deprotonated 5-chloro-6-hydroxypyridine-3-carboxylate anion

Experimental

Materials and methods

All chemicals are commercially available and were used as received without further purification. The elemental analyses were performed on a FLASH EA1112 elemental analyzer. The infrared spectra were recorded on a BRUKER TENSOR-27 spectrophotometer with pressed KBr pellets. The magnetic susceptibility measurements were carried out on polycrystalline samples on a Quantum Design MPMS-XL5 SQUID magnetometer. Diamagnetic corrections were estimated from Pascal's constants for all constituent atoms.

Synthetic procedures

A mixture of 5-Cl-6-HOPy-3-CO_2H (1.0 mmol), Ln_2O_3 (0.25 mmol), H_2(OX) (0.5 mmol) and 15 mL of H_2O in a Teflon-lined stainless steel autoclave (25 mL) was kept at 170 °C for 6 days. After the autoclave had cooled to room temperature over 10 h, light yellow block crystals of **1** (Ln = Dy, 75% yield based on Dy), or colourless block crystals of **2** (Ln = Gd, 68% yield based on Gd) were harvested. These crystals were washed with water and dried at ambient temperature.

Elemental analysis (%): Calc. for $C_{16}H_{12}Cl_2Dy_2N_2O_{17}$ (**1**): C, 21.35; H, 1.34; N, 3.11. Found: C, 21.40; H, 1.36; N 3.08. IR (KBr pellet, cm^{-1}): 3646(m), 3502(b, s), 3138(w), 3061(w), 3018(w), 2962(w), 2899(w), 1731(m), 1665(s), 1607(s), 1560(m), 1535(m), 1422(s), 1388(m), 1354(w), 1308(m), 1254(w), 1183(w), 1161(w), 1056(w), 950(w), 922(w), 888(w), 835(w), 803(m), 789(m), 718(m), 638(m), 595(w), 532(w), 497(w), 424(w).

Elemental analysis (%): Calc. for $C_{13}H_{24}Cl_2GdN_2O_{17}$ (**2**): C, 22.04; H, 3.41; N, 3.95. Found: C, 22.08; H, 2.45; N 3.90. IR (KBr pellet, cm^{-1}): 3367(b, s), 3201(b, s), 3143(m), 3063(m), 2980(m), 2901(w), 1649(s), 1569(m), 1536(m), 1421(s), 1386(m), 1314(m), 1248(w), 1186(w), 1159(w), 1057(w), 954(w), 919(w), 884(w), 834(w), 791(m), 717(m), 636(m), 595(w), 529(w), 498(w), 420(w).

Crystallography

A single crystal with dimensions of 0.16 × 0.34 × 0.41 mm^3 of **1**, and a single crystal with dimensions of 0.04 × 0.16 × 0.22 mm^3 of **2** were picked out to collect data on a Bruker SMART APEX-CCD diffractometer with *Mo-Kα* radiation (λ = 0.71073 Å) at 173(2) K. Empirical absorption corrections from φ scan were applied. Cell parameters were obtained by the global refinement of the positions of all collected reflections for two complexes, whose structures were solved by direct methods and refined by a full matrix least-squares technique based on F^2 using SHELXL 97 program.[9] All non-hydrogen atoms were refined anisotropically, and all hydrogen atoms were refined as riding atoms. Selected crystallographic data and structure determination parameters for both complexes are given in Table 1.

Table 1. Crystal data and structural refinement parameters for **1** and **2**.

	1	**2**
Chemical formula	$C_{16}H_{12}Cl_2Dy_2N_2O_{17}$	$C_{13}H_{24}Cl_2GdN_2O_{17}$
Formula weight	900.18	708.99
Crystal system	Orthorhombic	Monoclinic
Space group	*Pnma*	$P2_1/c$
a/Å	8.3451(17)	8.0109(16)
b/Å	19.104(4)	28.894(6)
c/Å	15.096(3)	11.816(4)
β/°	90	120.59(2)
V/$Å^3$	2406.7(9)	2354.4(10)
Z	4	4
T/K	173(2)	173(2)
λ(Mo-Kα)/Å	0.71073	0.71073
ρ_{calc}/g · cm^{-3}	2.484	1.999
μ(Mo-Kα)/mm^{-1}	6.472	3.128
ϑ range	2.99°≤θ≤ 27.48°	2.12°≤θ≤ 25.02°
Limiting indices	−10≤*h*≤10, −24≤*k*≤23, −19≤*l*≤19	−7≤*h*≤9, −33≤*k*≤34, −14≤*l*≤13
Reflections collected	15220	13291
Unique reflections	2837	4159
$R_1{}^a$ [$I > 2\sigma(I)$]	0.0303	0.0497
$_wR_2{}^b$ [$I > 2\sigma(I)$]	0.0726	0.1175
$R_1{}^a$ [all data]	0.0306	0.0541
$_wR_2{}^b$ [all data]	0.0728	0.1211
S	1.102	1.046

$^aR_1 = \sum||Fo|-|Fc|| / \sum|Fo|$, $^b{}_wR_2 = \sum\{[w(Fo^2-Fc^2)^2] / \sum[wFo^2]^2\}^{1/2}$

Results and discussion

Synthetic procedures

To avoid forming the lanthanide(III) oxalate precipitate directly, we adopted the hydrothermal reaction technique to synthesize the goal products, and Ln_2O_3 was used as the Ln^{3+} source, which could synchronously react with not only oxalic acid but also other organic acids to assembly new LnMOFs with mixed ligands.[7] As observed in the LnMOFs derived from 6-HOPy-3-CO_2H,[7a,7b] a new ligand, namely, the 1H-5-Cl-6-Opy-3-CO_2^- anion was generated through an autoisomerization of the single deprotonated 5-Cl-6-HOPy-3-CO_2^- anion from the enol into ketone form (scheme 1) during the hydrothermal syntheses of **1** and **2**. This new ligand works as an organic linker to construct complexes **1** and **2** along with the oxalate bridge. It is noteworthy that a higher hydrothermal temperature (170 °C) is necessary to produce complexes **1** and **2**, in comparison with the hydrothermal temperature (150 °C) for the LnMOFs derived from 6-HOPy-3-CO_2H.[7a,7b] Surprisingly, when 6-HOPy-3-CO_2H was used as the reactant instead of 5-Cl-6-HOPy-3-CO_2H, no any crystalline products could be yielded, which suggests that the chloride group in 5-Cl-6-HOPy-3-CO_2H plays a critical role in the hydrothermal synthesis of **1**.

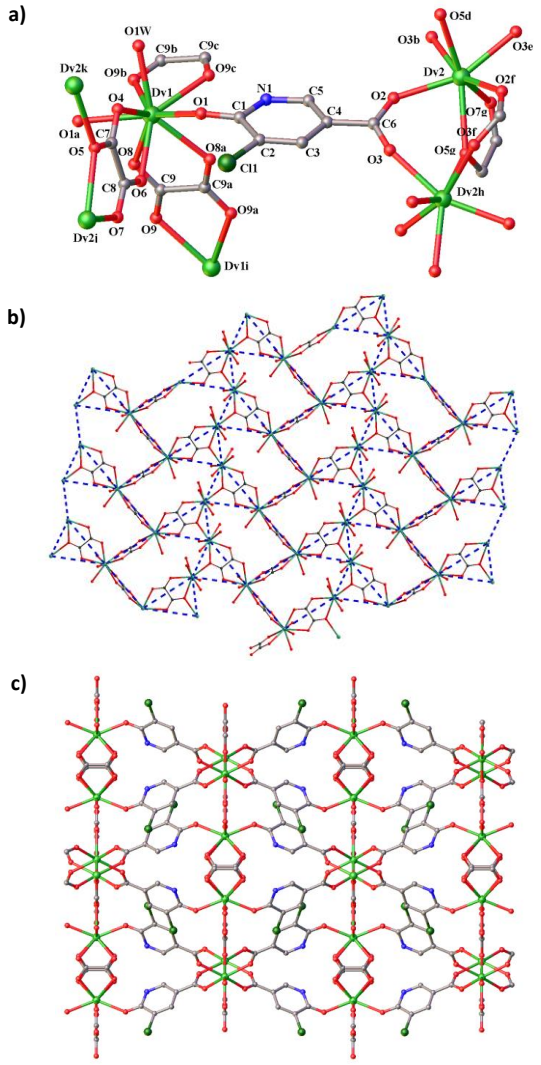

Fig. 1. Coordination environments of the Dy atoms in **1** (a), symmetry codes: a: x, 1/2−y, z; b: 1/2+x, y, 1/2−z; c: 1/2+x, 1/2−y, 1/2−z; d: 1−x, −1/2+y, 1−z; e: 1/2+x, −1/2−y, 1/2−z; f: x, −1/2−y, z; g: 1/2−x, −y, −1/2+z; h: −1/2+x, −1/2−y, 1/2−z; i: −1/2+x, 1/2−y, 1/2−z; j: 1/2−x, −y, 1/2+z; k: 1−x, 1/2+y, 1−z; dysprosium(III) oxalate layer (b); and 3D framework of **1** viewed along the *a*-axis (c).

Crystal structures

Complex **1** crystallizes in the space group *Pnma*. As shown in Fig. 1, the three-dimensional (3D) framework of **1** is composed of the dysprosium(III) oxalate layer and the 1H-5-Cl-6-HOpy-3-CO_2^- organic linker. There are two crystallographic independent dysprosium(III) atoms in **1** (Fig. 1a): the Dy1 atom has a nearly monocapped square-antiprism geometry, completed by six oxygen atoms from three oxalate anions, two ketone oxygen atoms from two 1H-5-Cl-6-HOpy-3-CO_2^- anions, and one oxygen atom from the coordinated hydrate molecule. The Dy2 atom is only seven-coordinated, showing a distorted pentagonal-bipyramidal geometry, which is bonded by two oxygen atoms from one oxalate anion, one oxygen atom from another oxalate anion, and four carboxylate oxygen atoms from four 1H-5-Cl-6-HOpy-3-CO_2^- anions. The Dy1-O bond distances (average 2.402 Å) are obviously larger than the Dy2-O bond lengths (mean 2.329 Å) (Table S1).

In the dysprosium(III) oxalate layer, the Dy^{3+} ions are connected with each other through the oxalate bridges in two types of coordination modes (Figs. 1a and 1b): the oxalate anion containing O8 acts as a bisbidentate coordination to two Dy1 atoms; while the oxalate unit containing O4 not only is a bisbidentate ligand to both the Dy1 atom and the Dy2 atom but also is a bismonodentate ligand to the neighbouring Dy2 atom. This dysprosium(III) oxalate layer belongs to a 4-connected network, with a Schälfli topology symbol of $(3^2.5^2)(3.5^3)$. Notably, such a layer represents a new structural paradigm of lanthanide oxalate.[3] To complete the 3D structure the dysprosium(III) oxalate layers are connected with each other by the bridging ligand 1H-5-Cl-6-HOpy-3-CO_2^- (Fig. 1c), which is generated by an autoisomerization from the enol form into the ketone form of the single deprotonated 5-Cl-6-HOPy-3-CO_2^- anion. The 1H-5-Cl-6-HOpy-3-CO_2^- ligand adopts a μ_3-bridging fashion to link three Dy^{3+} ions, through the *syn*–*syn* binding carboxylate group and the monodentate ketone oxygen atom. A similar coordination fashion was observed for the 1H-6-HOpy-3-CO_2^- anion in its corresponding LnMOFs.[7]

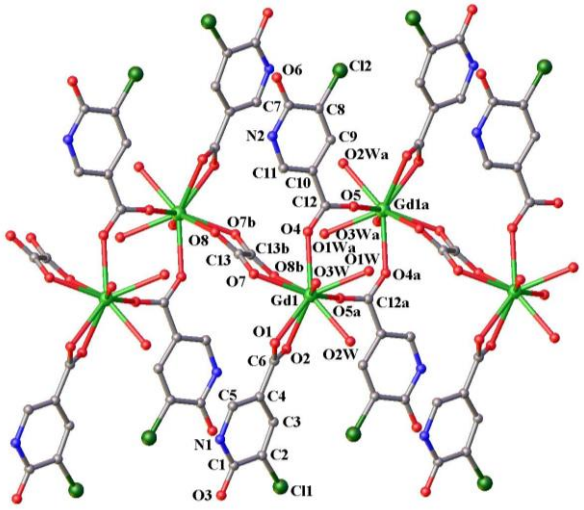

Fig. 2. 1D zigzag chain structure of **2** showing the coordination environment of the Gd atom, symmetry codes: a: −1−x, −y, 1−z; b: −x, −y, 1−z.

There are intermolecular hydrogen bonds between the solvent hydrate molecule and the coordinated water molecule (O1w…O2w 3.032 Å), between the solvent hydrate molecule and the oxalate oxygen atoms (O2w…O6 2.887 Å and O2w…O9 3.021 Å), and between the coordinated water molecule and the oxalate oxygen atom (O2w…O7 2.868 Å). In addition, there also exists a strong intramolecular hydrogen bond between the protonated pyridine nitrogen atom and the oxalate oxygen atom (N1…O9 2.760 Å). These hydrogen bonds are important to stabilize the crystal structure.

Very different from **1**, complex **2** shows a classical zigzag-chain structure in which the Gd atoms are connected with each other through alternatively arranged oxalate bridge and *syn*–*syn*

carboxylate double bridges (Fig. 2). Each Gd atom is coordinated by nine oxygen atoms, of which two are from the bis-chelating oxalate anion, two from the same carboxylato group of one 1H-5-Cl-6-HOpy-3-CO_2^- anion, two from two carboxylato groups of other two 1H-5-Cl-6-HOpy-3-CO_2^- anions, and three from three coordinated water molecules, generating a distorted monocapped square-antiprism geometry. The Gd-O bond distances [2.351(4)-2.572(5) Å] are in the normal range.[7b]

There are two kinds of 1H-5-Cl-6-HOpy-3-CO_2^- ligands in **2** according to the coordination modes: the first one uses two carboxylato oxygen atoms to bond the same Gd atom with the chelating mode, leaving the ketone O group free; the other one adopts a μ_2-bridging fashion to link two adjoining Gd atoms through the *syn*–*syn* binding carboxylate group, also leaving the ketone O atom free. In addition, the oxalate anion in **2** bridges two adjacent Gd atoms with the bisbidentate coordination mode.

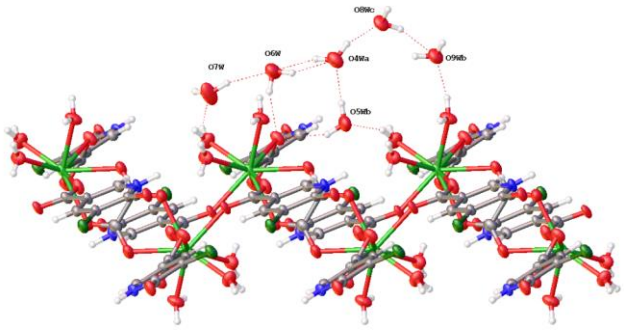

Fig. 3. The $(H_2O)_6$ cluster in **2** (formed by six labelled water molecules), symmetry codes: a: −1−x, −y, −z; b: 1+x, y, z; c: x, −1/2−y, −1/2+z.

There exist extensive intermolecular hydrogen bonds among the solvent hydrate molecules. Strikingly, a charming $(H_2O)_6$ supramolecular cluster, which exhibits a unique F shape, is observed in **2** (Fig. 3). The Ow···Ow separation within the hexameric water cluster ranges from 2.658 to 2.853 Å, which is comparable to 2.74 Å of ice I_c,[10] 2.76 Å of ice I_h,[11] and 2.85 Å of liquid water.[12] Obviously, this hexameric water cluster is not only different from the planar cyclic,[13] chair-like,[14] and boat-like[15] $(H_2O)_6$ supramolecular clusters characterized by X-ray crystallographic analysis, but also different from the energetically favourable cage, book, prism, boat and cyclic conformations supplied by theoretical studies.[16] This new type of hydrate cluster is also reminiscent of other beautiful hydrate supramolecular aggregates.[17] We believe that the specific microenvironments of the [Gd(1H-5-Cl-6-Opy-3-CO_2)$_2$(OX)$(H_2O)_3$] molecules support this unusual water hexamer, because it is further stabilized by the intermolecular hydrogen bonds between the solvent water molecule and the coordinated water molecule, between the solvent water molecule and the oxalate oxygen atom, and between the solvent water molecule and the carboxylate oxygen atom.

The above two coordination polymers' dimensions degressively vary from the 3D framework into the 1D chain, contrary to the trend observed in the LnMOFs derived from 6-HOPy-3-CO_2H,[7b] which can be ascribed to the lanthanide contraction effect.

Magnetic properties

Microcrystalline powdered samples of both complexes were used to measure their direct current (dc) magnetic susceptibilities in the temperature range of 2–300 K under an applied field of 1 kOe. As shown in Fig. 4a, the χT value at 300 K (28.17 cm^3Kmol^{-1}) is slightly smaller than that expected (28.34 cm^3Kmol^{-1}) for two Dy^{3+} non-interacting ions (S = 5/2, L = 5, $^6H_{15/2}$, g = 4/3). The χT product keeps almost invariable in the high temperature range, but falls abruptly as temperature further deceases below 50 K, reaching a minimum value of 21.56 cm^3Kmol^{-1} at 2 K. The $1/\chi$ versus T plot obeys the Curie–Weiss law, $1/\chi = (T-\vartheta)/C$, with the Curie constant C of 28.31 cm^3Kmol^{-1} and the Weiss constant ϑ of −1.16 K. The small negative ϑ value implies that the magnetic anisotropy and the thermal depopulation of the Dy^{3+} excited states (Stark sublevels of the $^6H_{15/2}$ state) rather than the intramolecular antiferromagnetic interaction should be the main reason for the decline of the χT value with decreased temperature. This magnetic anisotropy is also confirmed by the field dependence of the magnetization recorded at different temperatures, as shown in Fig. 4b, the produced M versus H/T curves are remarkably non-superimposed.

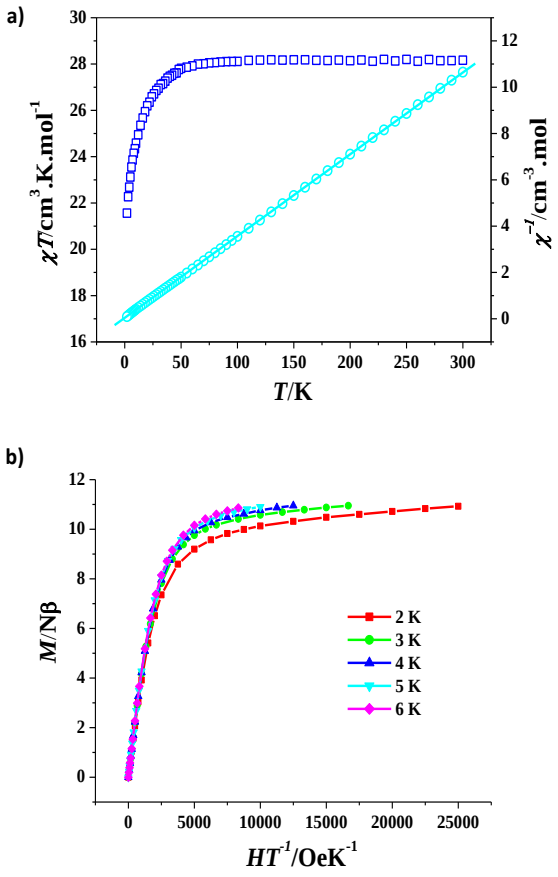

Fig. 4. Plots of χT versus T (□) and $1/\chi$ versus T (○) of **1**(a), the solid li represents the best theoretical fitting; M versus H/T plots at 2-6 K of **1** (b).

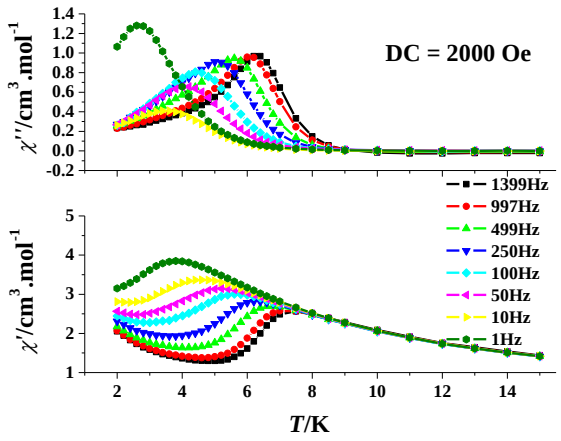

Fig. 5. Ac susceptibilities measured in a 2.5 Oe oscillating field with a 2 kOe dc field for **1**.

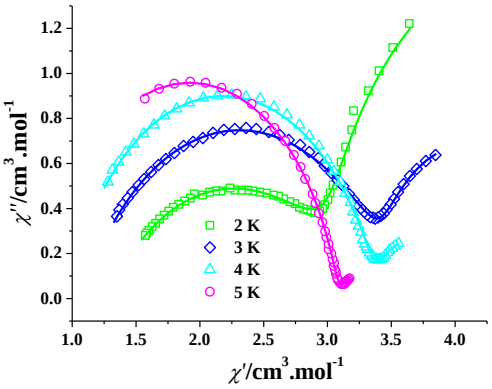

Fig. 6. Cole–Cole plots at 2–5 K for **1** (H_{dc} = 2 kOe and H_{ac} = 2.5 Oe). The solid lines represent the best fitting with the sum of two modified Debye functions.

In order to study magnetization dynamics of **1**, alternating-current (ac) magnetic susceptibility measurements were carried out in a 2.5 Oe oscillating field at different frequencies. When the static field was zero, no any out-of-phase (χ'') signals were detected (Fig. S1). However, after application of a dc field of 2000 Oe, both the χ' and χ'' signals of **1** are strongly frequency dependent below 9 K, and most importantly, peak shapes could be observed clearly (Fig. 5). These results indicate that the magnetic relaxation process of **1** is strongly influenced by quantum effects, and the 2000 Oe dc field effectively removes the ground-state degeneracy and thus induces the quantum-tunneling effects. A parameter $\phi = (\Delta T_f/T_f)/\Delta(\log f)$ (f is the frequency), is generally used to judge the nature of ac susceptibility frequency dependence to be superparamagnet ($\phi > 0.1$) or spin glass($\phi \approx 0.01$) behaviours.[18] The ϕ value of **1** was calculated to be 0.42, suggesting the SMM behaviours of **1**. The ac oscillating frequencies corresponding to the peak temperatures were presented as the form of ln(τ)-1/T plots (Fig. S2), which were then analysed using the Arrhenius law, $\tau = \tau_0 \exp(U_{eff}/kT)$ (here τ is the magnetization relaxation time), giving the U_{eff}/k value of 37.6 K and the τ_0 value of 3.5×10^{-6} s. The τ_0 value is in the normal range of 10×10^{-6}-10×10^{-11} s for the SMMs or the SIMs.[4-6]

To deeply explore the magnetic relaxation process of **1**, the frequency-dependent ac susceptibilities were determined at 2-5 K under a dc field of 2000 Oe, which are depicted in the format of χ'' versus χ' plots (Fig. 6), such Cole–Cole plots exhibit four hook-like curves in which the semicircular characteristic is still retained. These results indicate that there are two thermal magnetic relaxation processes: the left part of the Cole–Cole curve corresponds to the fast relaxation phase (FR), while the right part to the slow relaxation phase (SR). Such two-step thermal magnetic relaxation could be analyzed by the sum of two modified Debye functions(equ 1):[8b, 8c, 19]

$$\chi_{ac}(\omega) = \frac{\chi_2 - \chi_1}{1 + (i\omega\tau_2)^{(1-\alpha_2)}} + \frac{\chi_1 - \chi_0}{1 + (i\omega\tau_1)^{(1-\alpha_1)}} + \chi_0 \quad (1)$$

The results are listed in Table S2 and depicted as Fig. 6 and Figs. S3-S6. The α_1 values in the range of 0.00005-0.12 are obviously smaller than the coresponding α_2 values in the range of 0.59–0.19 at all four temperatures, suggesting that the FR phase has a relatively narrower distribution of the relaxation time with respect to the SR phase. As described above, there are two kinds of dysprosium(III) ions showing different coordination geometries in **1**, which may be is the main reason for **1** to display two steps of relaxation processes. Such a trend was also reported by other groups recently.[20] It should be noteworthy that complex **1** represents a rare example of 3D LnMOFs showing two steps of thermal magnetic relaxation processes. In addition, no any hysteresis effect can be observed in the M versus H plot of **1** at 1.9 K (Fig. S7).

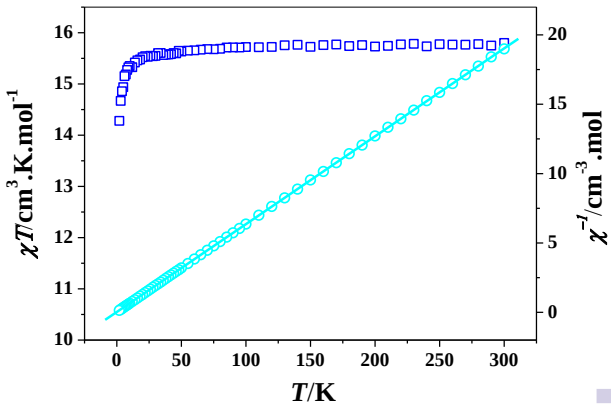

Fig. 7. Plots of χT versus T (□) and 1/χ versus T (○) of complex **2**, the solid line represents the best theoretical fitting.

For the isotropic gadolinium(III) complex **2**, the χT value at room temperature is 15.80 cm^3Kmol^{-1}(Fig. 7), in agreement with the spin-only value (15.76 cm^3Kmol^{-1}) for two noninteracting Gd ions (S = 7/2, L = 0, g = 2). Upon cooling, the observed χT product is almost invariable till 25 K, then falls fastly to reach a minimum value

of 14.28 cm^3Kmol^{-1} at 2.0 K, which is most likely ascribled to the weak antiferromagnetic interaction among gadolinium(III) ions and/or zero-field splitting. The magnetic susceptibility data in the whole temperature range of 2–300 K were fitted by the Curie–Weiss law, affording the ϑ value of −0.41 K and the *C* value of 15.79 cm^3Kmol^{-1}. The Curie constant *C* value corresponds to a *g* value of 2.0, while the small negative Weiss constant ϑ value confirms that the antiferromagnetic interaction among gadolinium(III) ions in **2** is very weak.

Conclusions

In summary, we have hydrothermally synthesized two novel lanthanide coordination polymers derived from 5-chloro-6-hydroxypyridine-3-carboxylic acid, in which oxalate acts as the co-ligand to bridge neighbouring lanthanide ions. A new ligand, 1H-5-Cl-6-HOpy-3-CO_2^- anion was generated *in situ* through an autoisomerization from the enol form into the ketone form of the single deprotonated 5-chloro-6-hydroxypyridine-3-carboxylic acid during the hydrothermal syntheses of two complexes. Complex **1** is a 3D metal-organic framework containing a unique dysprosium(III) oxalate layer, and the 1H-5-Cl-6-HOpy-3-CO_2^- anion works as the μ_3-bridge to link such layers. Complex **2** possesses a zigzag chain-like structure, in which the oxalate bridge and the *syn–syn* carboxylate double bridges from two 1H-5-Cl-6-HOpy-3-CO_2^- anions link the Gd atoms alternatively. Amazingly, a new type of $(H_2O)_6$ cluster, which displays a unique F shape, exists in the crystal structure of **2**. The remarkable structural difference between **1** and **2** could be ascribed to the lanthanide contraction effect. Interestingly, complex **1** is a field-induced SMM, displaying two steps of thermal magnetic relaxation processes. This work demonstrates that the structures of lanthanide coordination polymers can be greatly influenced by the lanthanide contraction effect, and the SMM behaviours may exist in lanthanide–organic frameworks, more such molecular materials are under way.

Acknowledgements

This work was supported by National Key Basic Research Program of China (2013CB933403), National Natural Science Foundation of China (21471154 and 91022014), and the Strategic Priority Research Program of the Chinese Academy of Sciences (XDB12010103).

Notes and references

1 (a) J. Kido and Y. Okamoto, *Chem. Rev.*, 2002, **102**, 2357; (b) N. Marques, A. Sella and J. Takats, *Chem. Rev.*, 2002, **102**, 2137; (c) M. N. Bochkarev, *Chem. Rev*., 2002, **102**, 2089; (d) K. Kuriki, Y. Koike and Y. Okamoto, *Chem. Rev.*, 2002, **102**, 2347; (e) H. Tsukube and S. Shinoda, *Chem. Rev.*, 2002, **102**, 2389; (f) N. Sabbatini, M. Guardigli and J.M. Lehn, *Coord. Chem. Rev.*, 1993, **123**, 201; (g) D. Parkar, *Coord. Chem. Rev.*, 2000, **205**, 109; (h) Y. Hasegawa and T. Nakanishi, *RSC Adv.*, 2015, **5**, 338.

2 J. Rocha, L. D. Carlos, F. A. A. Paza and D. Ananias, *Chem. Soc. Rev.*, 2011, **40**, 926.

3 (a) R. Vaidhyanathan, S. Natarajan and C. N. R. Rao, *Inorg. Chem.*, 2002, **41**, 4496; (b) L. Cañadillas-Delgado, J. Pasán, O. Fabelo, M. Hernández-Molina, F. Lloret, M. Julve and C. Ruiz-Pérez, *Inorg. Chem*., 2006, **45**, 10585; (c) B. Li,W. Gu, L.-Z. Zhang, J. Qu, Z.-P. Ma, X. Liu and D.-Z. Liao, *Inorg. Chem.*, 2006, **45**, 10425; (d) W.-H. Zhu, Z.-M. Wang and S. Gao, *Inorg. Chem.*, 2007, **46**, 1337; (e) M.-S. Liu, Q.-Y. Yu, Y.-P. Cai, C.-Y. Su, X.-M. Lin, X.-X. Zhou and J.-W. Cai, *Cryst. Growth Des.*, 2008, **8**, 4083; (f) Q.-F. Yang, Y. Yu, T.-Y. Song, J.-H. Yu, X. Zhang, J.-Q. Xu and T.-G. Wang, *CrystEngComm*, 2009, **11**, 1642; (g) Z.-P. Deng, W. Kang, L.-H. Huo, H. Zhao and S. Gao, *Dalton Trans*., 2010, **39**, 6276; (h) T.-F. Liu, W.j. Zhang, W.-H. Sun and R. Cao, *Inorg. Chem*., 2011, **50**, 5242; (h) H. Wang , S.-J. Liu, D. Tian, J.-M. Jia and T.-L. Hu, *Cryst. Growth Des.*, 2012, **12**, 3263; (i) X. Feng, X.-L. Ling, L. Liu, H.-L. Song, L.-Y. Wang, S.-W. Ng and B.-Y. Su, *Dalton Trans*., 2013, **42**, 10292; (j) A.-H. Yang, J.-Y. Zou, W.-M. Wang, X.-Y. Shi, H.-L. Gao, J.-Z. Cui and B. Zhao, *Inorg. Chem.*, 2014, **53**, 7092; (k) Y.-H. Zhang, X. Li, S. Song, H.-Y. Yang, D. Ma and Y.-H. Liu, *CrystEngComm*, 2014, **16**, 8390; (l) S. Natarajan and S. Mandal, *Angew. Chem. Int. Ed*., 2008, **47**, 4798.

4 R. Sessoli, D. Gatteschi, A. Caneschi and M. A. Novak, *Nature*, 1993, **365**, 141.

5 (a) G. Christou, D. Gatteschi, D. N. Hendrickson and R. Sessoli, *MRS Bull*., 2000, **25**, 66; (b) D. Gatteschi and R. Sessoli, *Angew. Chem. Int. Ed.*, 2003, **42**, 268; (c) G. Aromi and E. K. Brechin, *Struct. Bonding*, 2006, **122**, 1; (d) C. Benelli and D. Gatteschi, *Chem. Rev.*, 2002, **102**, 2369; (e) R. Bagai and G. Christou, *Chem. Soc. Rev.,* 2009, **38**, 1011; (f) G. E. Kostakis, A. M. Akoab and A. K. Powell, *Chem. Soc. Rev*., 2010, **39**, 2238; (g) L. M. C. Beltran and J. R. Long, *Acc. Chem. Res*., 2005, **38**, 325; (h) V. Chandrasekhar and B. Murugesapandian, *Acc. Chem. Res*., 2009, **42**, 1047; (i) R. Sessoli and A. K. Powell, *Coord. Chem. Rev*., 2009, **253**, 2328; (j) M. Murrie, *Chem. Soc. Rev.* 2010, **39**, 1986; (k) R. Vincent, S. Klyatskaya, M. Ruben, W. Wernsdorfer and F. Balestro, *Nature*, 2012, **488**, 357; (l) T. Komeda, H. Isshiki, J. Liu, Y.-F. Zhang, N. Lorente, K. Katoh, B. K. Breedlove and M. Yamashita, *Nat. Comm.,* 2011, **2**, 21. (m) D. N. Woodruff, R. E. P. Winpenny and R. A. Layfield, *Chem. Rev*., 2013, **113**, 5110; (n) B.-W. Wang, X.-Y. Wang, H.-L. Sun, S.-D. Jiang and S. Gao, *Philos. Trans. R. Soc. A*, 2013, **371**, 20120316; (o) K. Liu, W. Shi and P. Cheng, *Coord. Chem. Rev*., 2015, **289-290**, 74; (p) P. Zhang, Y.-N. Guo and J.k. Tang, *Coord. Chem. Rev*., 2013, **257**, 1728.

6 (a) D. Savard, P. H. Lin, T. J. Burchell, I. Korobkov, W. Wernsdorfer, R. Clérac and M. Murugesu, *Inorg. Chem*., 2009, **48**, 11748; (b) P. F. Shi, Y. Z. Zheng, X. Q. Zhao, G. Xiong, B. Zhao, F. F. Wan and P. Cheng, *Chem.–Eur. J*., 2012, **18**, 15086; (c) F. R. Fortea-Perez, J. Vallejo, M. Julve, F. Lloret, G. De Munno, D. Armentano and E. Pardo, *Inorg. Chem*., 2013, **52**, 4777; (d) X. Yi, K. Bernot, G. Calvez, C. Daiguebonne and O. Guillou, *Eur. J. Inorg. Chem.*, 2013, 5879; (e) M. Chen, E. C. Sañudo, E. Jiménez, S.-M. Fang, C.-S. Liu and M. Du, *Inorg. Chem*., 2014, **53**, 6708; (f) D.-D. Yin, Q. Chen, Y.-S. Meng, H. Sun, Y.-Q. Zhang and S. Gao, *Chem. Sci*., 2015, **6**, 3095; (g) X. Yi, G. Calvez, C. Daiguebonne, O. Guillou and Kevin Bernot, *Inorg. Chem*., 2015, **54**, 5213; (h) Q. Li and S. Du, *RSC Adv*., 2015, **5**, 9898; i) Q.-Y. Liu, Y.-L. Li, Y.-L. Wang, C.-M. Liu, L.-W. Ding and Y. Liu, *CrystEngComm*, 2014, **16**, 486; (j) C.-M. Liu, D.-Q. Zhang and D.-B. Zhu, *RSC Adv.*, 2014, **4**, 36053.

7 (a) C.-M. Liu, J.-L. Zuo, D.-Q. Zhang and D.-B. Zhu, *CrystEngComm*, 2008, **10**, 1674; (b) C.-M. Liu, M. Xiong, D.-Q. Zhang, M. Du and D.-B. Zhu, *Dalton Trans*., **2009**, 5666.

8 (a) C.-M. Liu, D.-Q. Zhang, X. Hao and D.-B. Zhu, *Cryst. Growth Des.*, 2012, **12**, 2948; (b) C.-M. Liu, D.-Q. Zhang and D.-B. Zhu, *Inorg. Chem.*, 2013, **52**, 8933; (c) C.-M. Liu, D.-Q.

Zhang and D. B. Zhu, *Dalton Trans*., 2013, **42**, 14813; (d) C.-M. Liu, D.-Q. Zhang and D. B. Zhu, *Dalton Trans.*, 2010, **39**, 11325; (e) C.-M. Liu, D.-Q. Zhang, X. Hao and D.-B. Zhu, *Chem.–Asian J*., 2014, **9**, 1847; (f) X.-L. Li, C.-L. Chen, Y.-L. Gao, C.-M. Liu, X.-L. Feng, Y.-H. Gui and S.-M. Fang, *Chem.–Eur. J.*, 2012, **18**, 14632

9 G. M. Sheldrick, SHELXL-97, *Program for refinement of crystal structures*, University of Göttingen, Germany, 1997.

10 L. J. Barbour, G. W. Orr and J. L. Atwood, *Nature*, 1998, **393**, 671.

11 M. Matsumoto, S. Saito and I. Ohmine, *Nature*, 2002, **416**, 409.

12 D. Eisenberg and W. Kauzmann, *The Structure and Properties of Water*, Oxford University Press, Oxford, UK, 1969.

13 J.N. Moorthy, R. Natarajan and P. Cenugophlan, *Angew. Chem. Int. Ed.*, 2002, **18**, 3417.

14 (a) C. Foces-Foses, F. H. Cano, M. Martinez-Ripoll, R. Faure, C. Roussel, R. M. Claramunt, C. Lopez, D. Sanz and J. Elguero, *Tetrahedron: Asymmetry,* 1990, **1**, 65; (b) R. Custelcean, C. Afloroaei, M. Vlassa and M. Polverejan, *Angew. Chem. Int. Ed.,* 2000, **39**, 3094.

15 K.-M. Park, R. Kuroda and T. Iwamoto, *Angew. Chem. Int. Ed.,* 1993, **32**, 884.

16 K. Liu, M.G. Brown, C. Carter, R.J. Saykally, J.K. Gregory and D.C. Clary, *Nature,* 1996, **381**, 501.

17 (a) R. Custelcean, C. Afloroaiei, M.Vlassa and M. Polverejan, *Angew. Chem. Int. Ed.,* 2000, **39**, 3094; (b) B.-Q. Ma, H.-L. Sun and S. Gao, *Angew. Chem. Int. Ed.,* 2004, **43**, 1374; (c) M. Henry, F. Taulelle, T. Loiseau, L. Beitone and G. Férey, *Chem. –Eur. J*., 2004, **10**, 1366; (d) M. Yoshizawa, T. Kusukawa, M. Kawano, T.Ohhara, I. Tanaka, K. Kurihara, N. Niimura and M. Fujita, *J. Am. Chem. Soc*., 2005, **127**, 2798; (e) P. S. Lakshminarayanan, E.Suresh and P. Ghosh, *Angew. Chem. Int. Ed.,* 2006, **45**, 3807; (f) M. Wei, C. He, W. Hua, C. Duan, S. Li and Q. Meng, *J. Am. Chem. Soc.,* 2006, **128**, 13318; (g) Q. H. Pan, J. Y. Li, K. E. Christensen, C. Bonneau, X. Y. Ren, L. Shi, J. L. Sun, X. D. Zou, G. H. Li, J. H. Yu and R. R. Xu, *Angew. Chem. Int. Ed*., 2008, **47**, 7868; (h) Y.-C. Qu, Z.-j. Lin and M.-L. Tong, *CrystEngComm,* 2010, **12**, 4020; (i) C.-M. Liu, D.-Q. Zhang, X. Hao and D.-B. Zhu, *Chem. –Eur. J.,* 2011, **17**, 12285.

18 J. A. Mydosh, *Spin Glasses, An Experimental Introduction*, Taylor and Francis, London, 1993.

19 (a) M. Grahl, J. Kotzler and I. Sessler, *J. Magn. Magn. Mater*., 1990, **90–91**, 187; (b) Y.-N. Guo, G.-F. Xu, P. Gamez, L. Zhao, S.-Y. Lin, R. Deng, J. Tang and H.-J. Zhang, *J. Am. Chem. Soc.*, 2010, **132**, 8538.

20 (a) Z. Sun, D. Ruiz, N. R. Dilley, M. Soler, J. Ribas,K. Folting, M. Brian Maple, G. Christou and D. N. Hendrickson, *Chem. Commun.*, 1999, 1973; (b) I. J. Hewitt, J. Tang, N. T. Madhu, C. E. Anson, Y. Lan, J. Luzon, M. Etienne, R. Sessoli and A. K. Powell, *Angew. Chem. Int. Ed.*, 2010, **49**, 6352; (c) Y.-X. Wang, W. Shi, H. Li, Y. Song, L. Fang, Y. Lan, A. K. Powell, W. Wernsdorfer, L. Ungur, L. F. Chibotaru, M. Shenc and P. Cheng, *Chem. Sci.*, 2012, **3**, 3366; (d) J. Long, F. Habib, P.-H. Lin, I. Korobkov, G. Enright, L. Ungur, W. Wernsdorfer, L. F. Chibotaru and M. Murugesu, *J. Am. Chem. Soc.*, 2011, **133**, 5319; (e) M.-X. Yao, Q. Zheng, F. Gao, Y.-Z. Li, Y. Song and J.-L. Zuo, *Dalton Trans.*, 2012, **41**, 13682; (f) K. Katoh, T. Kajiwara, M. Nakano, Y. Nakazawa, W. Wernsdorfer, N. Ishikawa, B. K. Breedlove and M. Yamashita, *Chem. –Eur. J.*, 2011, **17**, 117; (g) F. Gao, Y.-Y. Li, C.-M. Liu, Y.-Z. Li and J.-L. Zuo, *Dalton Trans.*, 2013, **42**, 11043; (h) S. K. Langley, N. F. Chilton, B. Moubaraki and K. S. Murray, *Inorg. Chem.*, 2013, **52**, 7183; (i) R. J. Blagg, L. Ungur, F. Tuna, J. Speak, P. Comar, D. Collison, W. Wernsdorfer, E. J. L. McInnes, L. F. Chibotaru and R. E. P. Winpenny, *Nat. Chem.*, 2013, **5**, 673; (j) S. Das, A. Dey, S. Biswas, E. Colacio and V. Chandrasekhar, *Inorg. Chem*., 2014, **53**, 3417.

Journal Name

ARTICLE

Graphical Abstract

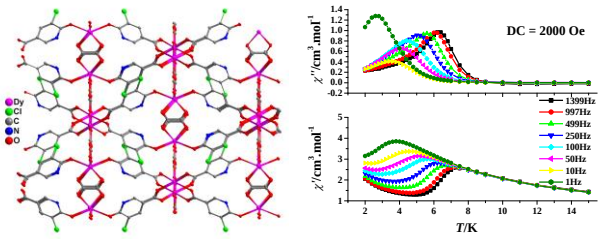

Two-step thermal magnetic relaxation was observed in a novel three-dimensional dysprosium(III) metal-organic framework.